Since January 2020 Elsevier has created a COVID-19 resource centre with free information in English and Mandarin on the novel coronavirus COVID-19. The COVID-19 resource centre is hosted on Elsevier Connect, the company's public news and information website.

Analytica Chimica Acta 1180 (2021) 338846

Contents lists available at ScienceDirect

Analytica Chimica Acta

journal homepage: www.elsevier.com/locate/aca

An ultrafast SARS-CoV-2 virus enrichment and extraction method compatible with multiple modalities for RNA detection

Leah M. Dignan [a, 1], Rachelle Turiello [a, *, 1], Tiffany R. Layne [a], Killian C. O'Connell [a], Jeff Hickey [b], Jeff Chapman [b], Melinda D. Poulter [c], James P. Landers [a, b, c, d, e]

[a] Departments of Chemistry, University of Virginia, Charlottesville, VA 22904, USA
[b] MicroGEM International PLC., Charlottesville, VA 22904, USA
[c] Departments of Pathology, University of Virginia, Charlottesville, VA 22904, USA
[d] Departments of Clinical Microbiology, University of Virginia, Charlottesville, VA 22904, USA
[e] Departments of Mechanical and Aerospace Engineering, University of Virginia, Charlottesville, VA 22904, USA

HIGHLIGHTS

- SARS-CoV-2 characterized by high transmission rates and pathogenicity worldwide.
- Diversification of sample preparation methods for SARS-CoV-2 is of paramount importance.
- Method for viral enrichment and enzymatic extraction of RNA in under 10 min.
- Eluates are compatible with downstream real-time PCR, LAMP, and RPA.

GRAPHICAL ABSTRACT

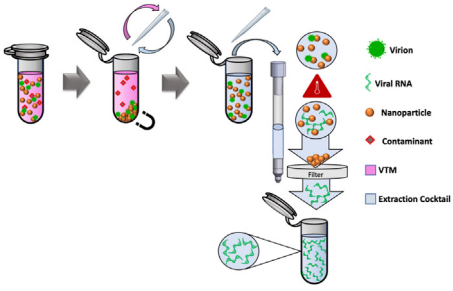

ARTICLE INFO

Article history:
Received 29 April 2021
Received in revised form
10 June 2021
Accepted 6 July 2021
Available online 13 July 2021

Keywords:
Enzymatic extraction
Affinity nanoparticles
Polymerase chain reaction (PCR)
Loop-mediated amplification (LAMP)
Recombinase polymerase amplification (RPA)
Severe acute respiratory syndrome coronavirus-2 (SARS-CoV-2)

ABSTRACT

Severe acute respiratory syndrome coronavirus 2 (SARS-CoV-2) is a zoonotic RNA virus characterized by high transmission rates and pathogenicity worldwide. Continued control of the COVID-19 pandemic requires the diversification of rapid, easy to use, sensitive, and portable methods for SARS-CoV-2 sample preparation and analysis. Here, we propose a method for SARS-CoV-2 viral enrichment and enzymatic extraction of RNA from clinically relevant matrices in under 10 min. This technique utilizes affinity-capture hydrogel particles to concentrate SARS-CoV-2 from solution, and leverages existing PDQeX technology for RNA isolation. Characterization of our method is accomplished with reverse transcription real-time polymerase chain reaction (RT-PCR) for relative, comparative RNA detection. In a double-blind study analyzing viral transport media (VTM) obtained from clinical nasopharyngeal swabs, our sample preparation method demonstrated both comparable results to a routinely used commercial extraction kit and 100% concordance with laboratory diagnoses. Compatibility of eluates with alternative forms of analysis was confirmed using microfluidic RT-PCR (μRT-PCR), recombinase polymerase amplification (RPA), and loop-mediated isothermal amplification (LAMP). The alternative methods explored here conveyed successful amplification from all RNA eluates originating from positive clinical samples. Finally, this method demonstrated high performance within a saliva matrix across a broad range of viral titers and dilutions up to 90% saliva matrix, and sets the stage for miniaturization to the microscale.

* Corresponding author.
E-mail addresses: rat3a@virginia.edu, rachelleturiello@gmail.com (R. Turiello).
[1] Both contributed equally to this manuscript.

https://doi.org/10.1016/j.aca.2021.338846
0003-2670/

1. Introduction

Severe acute respiratory syndrome coronavirus 2 (SARS-CoV-2) is a zoonotic RNA virus that can cause severe disease, specifically COVID-19, in humans [1]. Following its initial identification in December 2019, this novel betacoronavirus was quickly recognized by the World Health Organization (WHO) as a public health emergency of international concern [2]. The SARS-CoV-2 genome is comprised of positive-sense RNA encapsulated in a 50–200 nm diameter envelope possessing spike glycoproteins (S) that exhibit high affinity for host angiotensin-converting enzyme (ACE2) receptors to facilitate viral entry [3]. High transmission rates and pathogenicity contributed to a worldwide SARS-CoV-2 outbreak, making the development of rapid, simple, and sensitive diagnostic tools an urgent priority [4]. Continued epidemiological control requires diversification of methods for sample preparation and viral detection to allow for varied application, including widespread clinical testing, development of on-site diagnostics, and surveillance [5].

Current SARS-CoV-2 diagnostic assays rely on either serological tests to probe for the presence of antigen/antibodies or amplification-based detection of viral nucleic acids (NAs) in a variety of samples. Among these, real-time reverse transcriptase polymerase chain reaction (RT-PCR) is the most commonly employed method for 'confirmatory' viral detection and diagnosis. Boasting limits of RNA detection below 10 copies/μL, RT-PCR is widely recognized as a robust technique with high analytical sensitivity and specificity [6]. However, traditional real-time PCR detection relies heavily on laboratory instrumentation to measure fluorescence during continuous thermal cycling; these instruments must be operated by trained analysts and remain largely tethered to centralized laboratories [7].

Conversely, isothermal nucleic acid amplification tests (NAATs), including loop-mediated isothermal amplification (LAMP) and recombinase polymerase amplification (RPA), have generated interest for simple and rapid viral detection. Following the first description of LAMP-based detection of DNA and RNA targets by Notomi and coworkers in 2000, the technique has been widely adapted for simplified nucleic acid detection [8]. Further, the implementation of colorimetric indicators, such as hydroxy naphthol blue (HNB), has enabled simple, visual interpretation of amplification results [9]. Several groups have reported LAMP-based colorimetric assays for on-site SARS-CoV-2 detection [10–13]. Kellner et al. proposed a LAMP method for at-home diagnosis with limits of detection (LOD) of approximately 10 genomic copies of SARS-CoV-2 per reaction from crude patient samples [14]. RPA, first described by Piepenburg et al., permits isothermal exponential amplification of primer-defined loci of double stranded DNA by employing a recombinase protein [15,16]. Real-time RNA detection can also be achieved by incorporation of a reverse transcriptase RPA (RT-RPA) and a fluorescent probe [17]. One such recent method described by Behrmann et al. targeting the SARS-CoV-2 N gene enabled detection from clinical samples in only 7 min with 100% concordance to real-time RT-PCR [24]. Such isothermal strategies represent an emerging class of portable NAATs with potential to decrease strain on existing laboratory testing infrastructure [18–20].

Despite this rapidly expanding repertoire of NA amplification and detection techniques, challenges remain with regard to sample preparation. Purified RNA must first be isolated from complex biological matrices, which is generally achieved by viral lysis and silica-based solid phase extraction (SPE) [21]. While SPE methods are widely-accepted and effective, they are also expensive, time-consuming, labor-intensive, and not easily adapted to portable point-of-need devices. Furthermore, reliance on a narrow panel of gold-standard techniques may induce analytical bottlenecks, decreasing testing throughput, and ultimately hindering the control of viral spread [8]. As the pandemic continued, commercial nucleic acid preparation kits became supply-chain limited and existing laboratory infrastructure has been largely overwhelmed [22,23]. To enable the required expansion of testing capabilities, alternative analytical strategies must be implemented. One such strategy proposed by the United States Department of Human Health and Safety for surveillance in asymptomatic or low disease prevalence populations involves pooling samples from up to 20 individuals in a single test. In one analysis, 1191 samples required only 267 tests to detect 23 positive individuals [24,25]. Still, concerns exist regarding detection sensitivity from pooled samples; dilution of low titer samples could preclude their detection [23,24]. To prevent such false negative responses, Barclay et al. described a viral preconcentration method using paramagnetic affinity-capture hydrogel nanoparticles (Nanotrap®) to facilitate virion capture via interaction with surface spike proteins, and magnetic manipulation [26]. Inclusion of nanoparticle-based enrichment upstream of extraction appreciably improved the sensitivity of RT-PCR assays, successfully facilitating SARS-CoV-2 detection in low viral titer and pooled patient sample mimics [27].

Here, we describe a novel sample preparation method that combines nanoparticle-based enrichment with rapid, one-step enzymatic extraction to provide amplification-ready SARS-CoV-2 RNA from clinically-relevant matrices in under 10 min. Our approach leverages rnaGEM® kit chemistry centered on viral lysis by a thermophilic proteinase [28,29]. Adaptation of this extraction method to existing PDQeX technology simultaneously facilitates viral lysis, stabilization of RNA through the hydrolysis of RNases [30], and physical removal of capture nanoparticles in a single, hands-free step. Notably, RNA extracted in this manner does not require further purification prior to amplification, thus bypassing traditional SPE to enable more rapid sample preparation. Total analytical time is of primary importance during epidemiological outbreaks [31]; timely disease diagnosis and reporting are imperative for effective surveillance efforts and transmission prevention [32]. The method reported here is independent from supply-chain limited NA preparation kits, and is compatible with a variety of amplification/detection modalities. This not only facilitates immediate implementation across a variety of sectors, including 'surveillance' efforts, but also opens up possibilities for microfluidic integration and application to point-of-care diagnostics.

2. Materials & methods

2.1. Clinical SARS-CoV-2 sample preparation and analysis

Standard of care testing was performed according to the manufacturer's protocol with one of three available methods with emergency use authorization (EUA) from the FDA. These methods include the Abbott Alinity-m SARS-CoV-2 assay, the Abbott M2000 Real-Time SARS-CoV-2 Assay, and the Xpert Xpress SARS-CoV-2 Assay. Previously tested and refrigerated clinical samples in viral transport medium (VTM) were de-identified according to the IRB-approved protocol and assigned a study sample number. Each sample was vortexed for 10 s and a 600 μL to 1 mL aliquot was removed and placed in a labeled 2 mL screw-cap microcentrifuge tube. Aliquoted patient samples were inactivated by heat treatment for 30 min at 65 °C, transferred to a sealed zip-lock bag, and stored at −20 °C until further analysis.

2.2. Enriched rnaGEM extraction and analysis

Patient samples were previously analyzed by real-time RT-PCR

in the clinical laboratory at the University of Virginia Health System for diagnostic purposes. Here, any sample received with a clinically-assigned C_t value was considered clinically-positive. Clinical C_t values were also used to infer comparative viral titers. The two in-tube RNA isolation methods compared herein are referred to as either *conventional,* or *enriched rnaGEM* extractions. In conventional extractions, RNA was isolated from 250 μL of inactivated patient sample using the RNeasy Mini Kit (Qiagen, Valencia, CA, USA) with a DNase I treatment (New England Biolabs, Ipswich, MA, USA) according to manufacturer's instructions. Enriched rnaGEM extractions include a pre-concentration step in which 25 μL Nanotrap Magnetic Virus Particles (CERES Nanosciences, Inc. Manassas, VA, USA) were mixed with 250 μL of heat-inactivated patient sample. Following a brief incubation, the particles were magnetically separated and the supernatant was removed. Nanotrap particles were resuspended in a rnaGEM cocktail comprised of 44 μL water, 5 μL BLUE buffer, and 1 μL rnaGEM enzyme solution. Following incubation for 10 min at 75 °C and 5 min at 95 °C in a thermal cycler, the particles were again separated magnetically and the supernatant RNA solution was collected and retained (Fig. 1A). RNA extracts were stored at −80 °C until analysis.

2.3. RT-PCR conditions

Real-time RT-PCR nucleic acid detection of SARS-CoV-2 leveraged the Centers for Disease Control and Prevention (CDC) assay developed under an emergency use authorization (EUA) in February 2020 [33]. Ct values obtained via real-time RT-PCR were used for relative quantification of SARS-CoV-2 RNA to assess the performance of upstream sample preparation conditions, given that more successful extraction would result in faster amplification (Fig. 1B). Each 20 μL reaction was composed of 5 μL TaqPath™ 1-Step RT-qPCR Master Mix, CG (Thermo Fisher Scientific, Waltham, MA, USA), 1.5 μL SARS-CoV-2 (2019-nCoV) CDC RUO N1 primer-probe mix (Integrated DNA Technologies, Coralville, IA, USA), 8.5 μL PCR-grade water (Molecular Biologicals International, Inc.), and 5 μL of extracted viral RNA. The 2019-nCoV_N_Positive Control plasmid (Integrated DNA Technologies) was used for positive controls. Samples were run in duplicate on a MyGo Pro real-time PCR instrument with detection in the FAM channel (IT-IS Life Science Ltd., Dublin, Ireland). Initial assay conditions included reverse transcription at 50 °C for 900 s, a 95 °C step for 180 s, and 40 cycles of denaturation and annealing (95 °C for 3 s and 55 °C for 30 s). Upon further optimization, reverse transcription was shortened to 60 s and the annealing temperature was increased to 60 °C. For all conditions, ramp rates up and down were 5 °C/s and 4 °C/s, respectively. We defined successful detection simply as observed amplification prior to the cut-off cycle described for the CDC RUO kit ($C_t = 40$).

2.4. Adaptation to the PDQeX platform

For RNA extractions using the PDQeX platform, 250 μL of sample was mixed with 25 μL of magnetic Nanotrap particles. The particles were magnetically separated and the supernatant was removed. For 50 μL total volume extractions without a DNase treatment, Nanotrap particles were resuspended in 44 μL water, 5 μL BLUE buffer, and 1 μL rnaGEM. Those 50 μL extractions with a DNase treatment included 38 μL water, 5 μL BLUE buffer, 1 μL rnaGEM 5 μL dsDNAse buffer, and 1 μL HL-dsDNase (ArcticZymes Technologies ASA, Tromsoe, Norway). For 100 μL total volume extractions, all reagent volumes were doubled. The Nanotrap particle suspensions were transferred to PDQeX long-read tubes, inserted into the associated instrument (MicroGEM International PLC), and heated directly to 95 °C for 5 min. RNA eluates were collected in 0.2 mL PCR tubes and stored at −80 °C until analysis.

2.5. Double-blind study: qualitative differentiation between clinical positives and negatives

Using a double-blind setup to prevent confirmational bias, a third party randomly selected clinical negative and positive samples, prepared aliquots for testing with no identifying information, and randomly assigned a letter (A − J) to each sample. The randomized sample tubes were transferred to a researcher for RNA isolation in 100 μL using the PDQeX system. Extracts were amplified (RT-PCR) by a second researcher. Researchers responsible for sample extraction and amplification proceeded without knowledge of sample identities until the results were analyzed and compared to known clinical results.

2.6. Fabrication and use of a microfluidic device for RT-PCR

Centrifugally-driven microfluidic devices for real-time RT-PCR were fabricated according to the print-cut-laminate (PCL) method, previously published by Thompson et al. [34] The architecture was designed using AutoCAD 2019 software (Autodesk, Inc., Mill Valley, CA, USA), then ablated into five polyethylene terephthalate (PeT) layers (Film Source, Inc. Maryland Heights, MO, USA) using a CO_2 laser (VLS3.50, Universal® Laser Systems, Scottsdale, AZ, USA). The fluidic layers (2 and 4) were coated on both sides with a heat sensitive adhesive (EL-7970-39, Adhesives Research, Inc. Glen Rock, PA, USA) [35]. An intervening layer of black PeT (Lumirror* X30, Toray Industries, Inc. Chhuo-ku Tokyo, Japan) prevented flow between discrete fluidic layers prior to laser valving [36]. All five layers were bonded together using an office laminator (UltraLAM

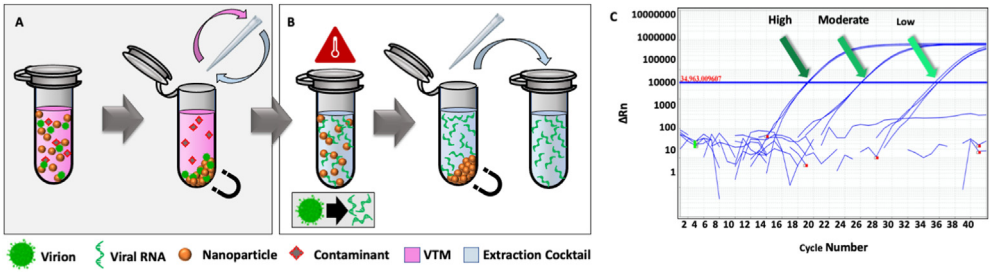

Fig. 1. Workflow for in-tube viral preconcentration and extraction of SARS-CoV-2 RNA. (A) SARS-CoV-2 virions were preconcentrated from viral transport medium (VTM) using paramagnetic capture particles. Following adsorption of the virion to the capture particles, they were collected magnetically and the supernatant VTM was removed. (B) The capture particles were re-suspended in rnaGEM extraction cocktail and heated to liberate viral RNA. Following a second magnetic immobilization step, the purified RNA supernatant was transferred to a second tube. (C) A representative amplification plot from RT-PCR amplification of extracted RNA. Such amplification techniques were used to characterize extraction and ultimately detect SARS-CoV-2.

250B, Akiles Products, Inc. Mira Loma, CA, USA). If increased chamber volume was required, laser-ablated polymethyl methacrylate (PMMA) components were adhered to the device surface using pressure sensitive adhesive (ARcare 7876, Adhesives Research, Inc.). A 20 μL reaction (prepared as described in 2.3) was pipetted into a loading chamber. The associated instrumentation for fluidic and temperature control has been described in detail elsewhere [37]. Briefly, a downstream valve was opened via laser irradiation and a brushed DC spin motor was used to centrifugally pump the fluid into the PCR chamber (3000 rpm, 30 s). Using an integrated dual-Peltier system, the reaction was incubated at 50 °C for 60 s, heated to 95 °C for 180 s, then underwent 40 cycles of 95 °C for 3 s and 60 °C for 30 s. The 2019-nCoV_N_Positive Control plasmid (1000 copies/μL) (Integrated DNA Technologies) again served as a positive reference material. No template controls and unamplified PCR reaction/2019-nCoV_N_Positive Control plasmid (Integrated DNA Technologies) were also included. Off-disc electrophoretic detection was achieved using a DNA chip in the Bioanalyzer 2100 (Agilent Technologies, Santa Clara, CA, USA).

2.7. One-step reverse transcription and recombinase polymerase amplification

A lyophilized pellet containing RPA reagents from the TwistAmp© Exo Kit (TwistDx™ Ltd. San Diego, CA, USA) was rehydrated in a total volume of 42.5 μL comprised of 29.5 μL TwistAmp Primer Free Rehydration buffer, 0.13 μM Exo-IQ probe (Eurofins Genomics LLC, Louisville, KY, USA), 10 U/μL ProtoScript II reverse transcriptase (Invitrogen, Carlsbad, CA, USA), 0.25 U/μL thermostable RNase H (New England Biolabs), 0.44 μM each SARS_RPA_F1 and SARS_RPA_R1 primers [38] (Eurofins Genomics LLC, Louisville, KY, USA), and 6.2 μL PCR-grade water. Each 25 μL reaction was comprised of 21.25 μL of the above mixture, 2.5 μL extracted sample and 14 nM magnesium acetate (MgOAc) (TwistDx™). The RNA extract and MqOAc were added, spatially separated, to the tube lid. Following brief centrifugation to start the RT-RPA reaction, the tubes were placed in a TS16-ISO instrument (Axxin, Fairfield, Victoria, Australia), preheated to 42 °C. Fluorescence was monitored within the FAM channel at 20% LED level. After 300 s, the samples were removed from the instrument, briefly vortexed and centrifuged, then returned for further incubation (1620 s). A threshold for amplification (618.619 RFU) was established three standard deviations above the mean fluorescence output of the NTCs throughout the assay duration.

2.8. Loop-mediated isothermal amplification with colorimetric detection

RT-LAMP reactions included 3.25 μL PCR-grade water, 6.25 μL 2x WarmStart master mix (New England Biolabs), 120 μM hydroxynaphthol blue (HNB), 1.25 μL sample, and 1.25 μL primer mix constructed with previously published primer sequences [10]. The primer mix contained 2 μM each F3 and B3 primers, 8 μM LF and LB primers, and 16 μM FIP and BIP primers. Triplicate no template and positive controls of the 2019-nCoV_N_Positive Control plasmid (Integrated DNA Technologies) at 1000, 100, and 10 copies/μL were included. RT-LAMP was performed at 63 °C for 60 min with a subsequent heat-kill step (95 °C, 1 min). Images of the tubes were captured using a Huawei smartphone at 0, 30, and 60 min; amplification was indicated by a colorimetric change of the reaction mixture from purple to blue, confirmed empirically using ImageJ software [39,40]. At each timepoint, the hue measured from a 15-pixel circular crop of each reaction was averaged across replicates. To objectively differentiate between positive and negative responses, a hue threshold (169.52 A U.) was established three standard deviations below the mean hue of all sample replicates before the reaction was allowed to proceed (time = 0). Any samples with measured hue values below this threshold, in the blue range, were considered positive for SARS-CoV-2.

2.9. Extraction of RNA from saliva samples

A solution of 10X phosphate-buffered saline (PBS) was prepared by dissolving 3.2073 g NaCl, 0.0807 g KCl, 0.5678 g Na_2HPO_4, and 0.0978 g KH_2PO_4 in 40 mL in molecular biology grade water (Fisher Scientific) and adjusting the pH to 7.35 with NaOH. Saliva dilution buffer was created by mixing 200 μL 10X PBS, 1400 μL molecular biology grade water (Fisher Scientific), and 400 μL BLUE buffer (MicroGEM International, PLC.). Saliva was diluted in this buffer in a 1:3 ratio. VTM from clinical samples was serially diluted in the resultant mixture prior to PDQeX extraction.

3. Results and discussion

3.1. Evaluation of the enriched rnaGEM approach

Besides clinical diagnosis alone, real-time RT-PCR may also be used as an analytical tool to examine the success of upstream nucleic acid preparation techniques. Given that C_t values are measured relative to target concentration, more successful nucleic acid extraction would yield higher levels of liberated RNA, thus promoting more rapid amplification. This principle is leveraged here to directly compare C_t values obtained from amplification of RNA extracted from clinically-positive SARS-CoV-2 samples in parallel using the proposed technique and a conventional, commercial method.

To characterize RNA extraction performance across a range of viral titers, three positive clinical samples with comparatively low, moderate, and high concentrations were analyzed. SARS-CoV-2 RNA was detected in all extracts with excellent concordance of resultant C_t values across methods. Clinical laboratories only report a qualitative yes/no response to practitioners to provide patient diagnoses. Since C_t values are for research purposes only, the minor (1−2 cycle) difference between the proposed and gold standard methods has negligible practical import. Conversely, the minimized time and labor requirements of the proposed method do stand to make a real impact in facilitating rapid and accurate clinical diagnosis of SARS-CoV-2 from patient samples.

To better compare our RNA extraction strategy to commercial methods, we analyzed all extracts used above at 5X, 10X, and 20X dilutions (Fig. 2) [26]. Overall, C_t values from parallel extracts were concordant. At each dilution of the moderate titer extract, the C_t values were within approximately one unit of each other across methods and viral RNA was detected in all dilutions, down to 20X (Fig. 2B). Similar trends were observed in analysis of the low viral titer sample with a single discrepancy, wherein the 20X dilution of the enriched rnaGEM extract exhibited no amplification but the parallel commercially extract dilution did (Fig. 2A). However, given the C_t value of the neat extract approached the cut-off cycle, we hypothesized that the concentrations of viral RNA in subsequent dilutions were likely in the stochastic regime, and ostensibly distribution of RNA in solution was inhomogeneous, failing to adhere to a normal distribution [41]. This theory was supported by failed amplification in one replicate of the 10X dilution of the commercial kit extract; given the observed amplification at 20X. Therefore, we concluded the methods performed comparably.

The most pronounced difference across methods was observed in the lowest C_t, or highest relative titer, sample (Fig. 2C). Although RNA obtained via enriched rnaGEM extraction was readily detected with C_t values of 20 ± 2 units in all dilutions, the values of

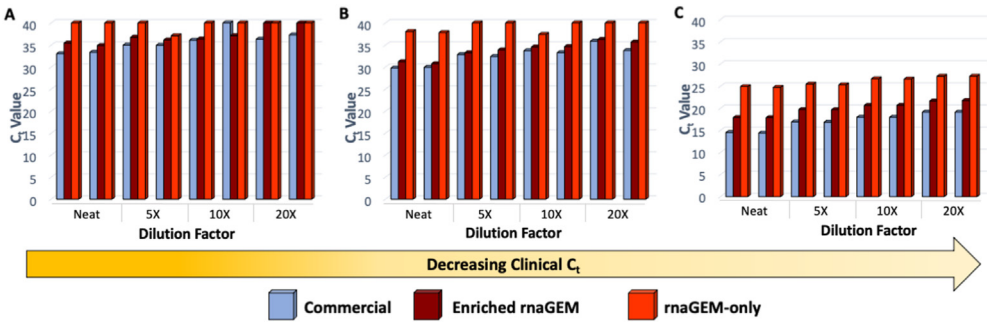

Fig. 2. Comparison of rnaGEM extraction methods with a commercial kit. SARS-CoV-2 RNA was extracted from known positive clinical samples in parallel using two methods - a commercial solid phase spin-basket kit, and rnaGEM extractions with viral preconcentration. Three samples with comparatively (A) high, (B) moderate, and (C) low Ct values were selected for comparison. Extracts were analyzed neat and serially diluted at factors of 5X, 10X, and 20X, each in duplicate. Ct values obtained from the enriched rnaGEM extracts were only slightly higher than extracts obtained using the commercial kit.

commercial extracts were ~3 cycles lower. A similar phenomenon was observed by Barclay et al., who suspected viral saturation of the nanoparticles at very high titers [22]; virions were likely sterically prevented from binding with the particles and were lost in the discarded supernatant prior to extraction. Still, Barclay et al. suggests that nanoparticle saturation does not affect the utility of enrichment-aided extractions since it does not prevent qualitative SARS-CoV-2 identification [22]. We believe this to be especially true as it pertains to high titer samples such as the one in question, since regardless of extraction method, amplification occurred well below the cut-off cycle and SARS-CoV-2 was readily detected.

We would add that the use of nanoparticle enrichment removes free RNA not contained in a viral envelope, known to persist in sample matrices well beyond patient infectivity [42]. Column-based methods are unable to differentiate RNA from infectious virus and naked RNA, thus confounding PCR-based diagnostics and efforts by public health officials to determine key metrics, such as required quarantine duration [42]. Since our method uses nanoparticle-based viral enrichment upstream of virion lysis, free, non-infectious RNA is not retained, potentially providing more accurate, useful information regarding patient infectivity.

3.2. Adaptation to the PDQeX platform

Given that high labor and time demands are principal drawbacks of existing RNA extraction methods, we sought to streamline our enriched rnaGEM method by leveraging specialized PDQeX technology. A single-temperature heating step induced enzymatic viral lysis, RNA extraction, elimination of RNases, and physical separation of the capture particles from the eluate. Simultaneous constriction of the PDQeX tube's inner heat-shrink layer and actuation of the heat burst valve below the sample reservoir forced fluid through an on-board filter into a collection tube while retaining the capture particles (Fig. 3A–B). To assess the effect of the platform on extraction performance, RNA was isolated from parallel aliquots of 3 clinical positives both using PDQeX and in-tube (thermal cycler) methods. Subsequent real-time RT-PCR analysis indicated comparable amplification across platforms, although C_t values were consistently 1–2 cycles lower following PDQeX extraction (Fig. 3C). The limited sample size in these proof-of-concept studies prevented conclusively alleging the PDQeX performance was superior, but the methods are certainly comparable. However, the PDQeX method supplanted several sequential manual steps with a single automated process, thereby decreasing variability and required analyst time.

To enable increased testing of a given extract, it was desirable to increase the elution volume, although this would inevitably dilute RNA. However, exploration of the effect of doubling the elution volume from 50 to 100 μL resulted in similar amplification of RNA extracted in parallel from 3 clinical positives. Resultant C_t values obtained from all three neat extracts and dilutions down to 20X were exhibited roughly one-unit differences and, therefore, comparable RNA concentrations (Fig. S1). Finally, a DNase was incorporated since the presence of genomic DNA (gDNA) is known to promote false positive real-time RT-PCR results by facilitating non-specific amplification and background fluorescence [43,44]. The DNase and associated buffer were added as part of the rnaGEM extraction cocktail; no additional steps were added to the extraction workflow. Although DNase treatments have been shown to decrease RNA yield [45,46], parallel extractions from clinical samples with and without DNase suggest that its inclusion was not detrimental to SARS-CoV-2 detection (Fig. S2). The optimal method for practical preparation of SARS-CoV-2 RNA used in all further studies was 100 μL total enriched rnaGEM PDQeX extractions with a DNase treatment.

3.3. Decreasing RT-PCR time

Despite widespread use of real-time RT-PCR for diagnosis and surveillance efforts, its lengthy sample-to-result interval, typically between 24 and 48 h due to workflow constraints, creates delays in reporting [31]. To shorten turnaround times, we evaluated changes to thermal cycling parameters and characterized their purported effect on detection of the CDC positive reference plasmid and enriched rnaGEM extracts.

Ramp rates were increased from 1.6 °C/s (per manufacturer's recommendation) between the cycle denaturation and annealing/extension steps to the maximal values permitted by the instrument software of 5 °C/s up and 4 °C/s down. The increased rates resulted in a 64% decrease in required ramping time during cycling, which equates to a 21-min difference, from over 57 min—~36 min. Importantly, across three different plasmid concentrations, analysis of the C_t values at each temperature indicated minimal effect on assay performance (Fig. S3). Subsequently, the cycle annealing temperature was increased from 55 °C to 60 °C, decreasing the temperature differential that must be overcome each cycle. Notably, at all three plasmid concentrations, increasing the annealing temperature decreased total assay time by approximately 2 min with minimal change in Ct values (Fig. S4). Using enriched rnaGEM extracts, the reverse transcription dwell time was decreased significantly from 15 min (manufacturer's recommendation) to 1 min. Parallel extracts from clinical samples were evaluated at both reverse transcription intervals and showed comparable amplification (Fig. S5). In total, by increasing the cycle

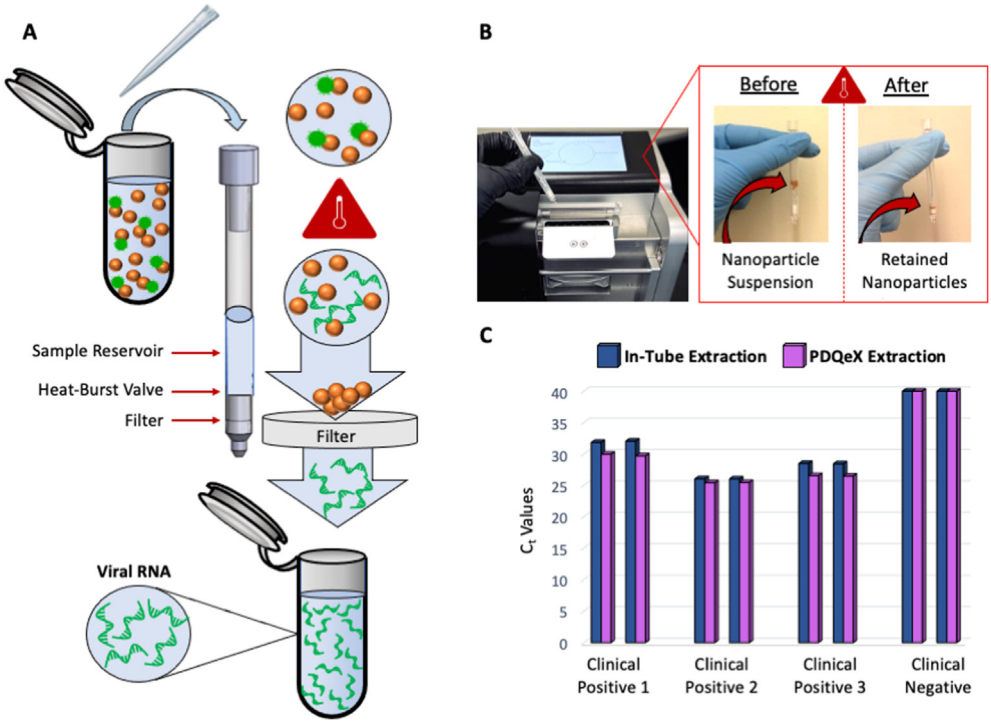

Fig. 3. Adaptation of the extraction protocol to PDQeX method. (A) Following in-tube viral preconcentration, the capture particle suspension in rnaGEM cocktail was transferred to a PDQeX tube. Incubation induced the inner walls of the tube to shrink and the heat-burst valve below the sample reservoir to be actuated, forcing the purified RNA solution through an on-board filter and into a final collection tube. (B) PDQeX instrument with inset images depicting the PDQeX tube before and after incubation. The capture particles are retained by the filter, supplanting the second manual magnetic step required in the in-tube protocol. (C) Comparison of the Ct values obtained from RT-PCR following parallel enriched rnaGEM extractions from four clinical samples (three positive and one negative) in-tube versus the PDQeX. Both methods performed comparably; across all three clinical positives and replicates, RNA amplification occurred ~1–2 cycles sooner. Each sample was analyzed in duplicate.

annealing temperature, using more rapid ramp rates, and decreasing the dwell time associated with reverse transcription, the total assay time required for SARS-CoV-2 was decreased by ~37 min, which could increase laboratory throughput and testing capabilities, and permit more rapid diagnoses and effective surveillance.

3.4. Double-blind study

We evaluated the accuracy of our extraction method with rapid RT-PCR analysis by testing patient samples in a double-blind format to avoid confirmational bias. Given the goal of providing a method for surveillance and transmission control, all positive samples in the selection pool had clinical C_t values below 32 since the likelihood of infectivity above this threshold is low [42]. Downstream RT-PCR showed amplification in both replicates of five of the ten deidentified samples (Fig. 4A); direct comparison of the experimental and clinical laboratory results illustrated the same outcome across methods for each sample (Fig. 4B). The five samples where SARS-CoV-2 viral RNA was detected (B, C, F, H, and I) corresponded to the five clinical positives selected, whereas the extracts that did not exhibit amplification (A, D, E, G, and J) were negative in the clinical laboratory. Our results exhibited 100% concordance with clinical laboratory analysis, demonstrating the ability of our sample preparation to concentrate and isolate SARS-CoV-2 from patient samples and provide accurate results by RT-PCR.

3.5. Compatibility with alternative amplification methods

Diversification of methods for SARS-CoV-2 detection will continue to elicit rapid, simple, and portable systems for on-site testing. With this in mind, eluates produced by our method were tested with microfluidic PCR, RPA, and LAMP using primers and probes from the literature [10,38]

3.5.1. Microfluidic PCR

Microfluidic systems offer portable alternatives that boast several advantages over conventional benchtop methods, including ease of use by nontechnical personnel, shortened analytical times, and enclosed formats [47,48]. Importantly, microfluidic platforms allow for more rapid thermal cycling than possible in-tube due to increased surface area to volume ratio that promotes more efficient heat transfer [49]. Therefore, adopting a microfluidic PCR (μPCR) approach has the potential to significantly decrease the sample-to-answer interval.

We demonstrated the direct compatibility of enriched rnaGEM extracted RNA with μPCR on a centrifugally-driven microdevice. Briefly, an individual reaction was flowed into a PCR chamber for thermal cycling (Fig. 5A–C). Off-disc electrophoretic detection of amplicons of the three positive clinical samples showed distinct peaks at ~78 base pairs, which corresponded to the size of the intended SARS-CoV-2 N1 target amplicon (Fig. 5D); all electropherograms obtained from negative extracts of clinical samples and negative controls did not exhibit this peak. These results indicate on-target μPCR amplification and detection of and SARS-CoV-2 RNA (Fig. 5D and S6) with both reverse transcription and amplification completed in a total of ~30 min. However, the PCR chamber had a depth of only ~500 μm, while the surface area directly in contact with the Peltier's was approximately 68 mm^2. This high surface area to volume ratio, coupled with the improved heat transfer properties inherent to the microscale, introduce the possibility to further reduce analysis time through more rapid cycling [49].

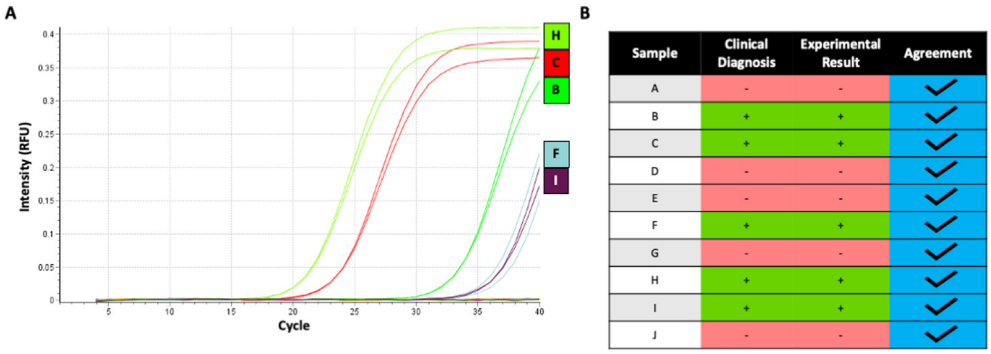

Fig. 4. Qualitative double-blind study to evaluate the sample preparation method. (A) RT-PCR amplification plot depicting clinical samples selected by a third party and deidentified prior to enriched rnaGEM extractions. SARS-CoV-2 RNA was detected in five of the ten samples analyzed (B, C, F, H, and I). The positive control (data not shown) had Ct values of 29.56 and 29.66, and the NTCs did not exhibit amplification. (B) A graphical representation of concordance between experimental results and clinical designations is shown. These results demonstrate 100% agreement of experimental results with clinical diagnoses of the ten deidentified patient samples evaluated in the double-blind study. Each sample was analyzed in duplicate.

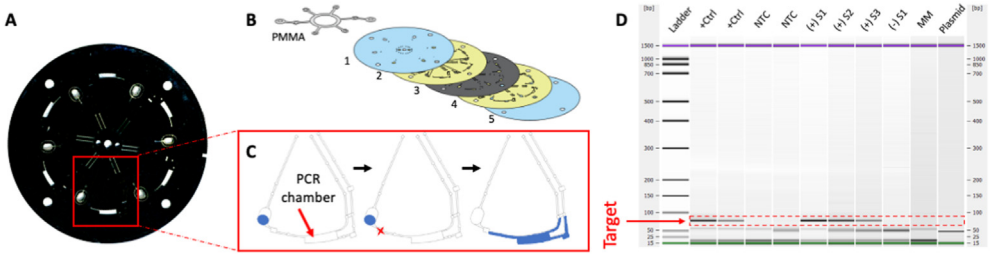

Fig. 5. Compatibility of extracted RNA with microfluidic PCR. (A) Image of 6-plex print-cut-laminate centrifugal microfluidic device designed for amplification of the SARS-CoV-2 extract. (B) Depiction of the five PeT layers used to construct the device, comprised of clear PeT capping layers (1 + 5), HSA-coated fluidic layers (2 + 4), and the black PeT (bPeT) valving layer (3). (C) Microfluidic architecture used for on-disc μPCR; the sample (blue) was introduced to a loading chamber, centrifugally pumped into the PCR chamber following laser valve actuation, and heated using a dual-Peltier system and analogous thermal cycling conditions to the optimized in-tube protocol. (D) Gel-image rendering of electropherograms obtained from fluorescent gel-based capillary electrophoresis of amplicons obtained from on-disc PCR. The target amplicon (~78 bp) was detected in both positive control (plasmid, 1000 copies/uL) samples and all clinical positives (neat VTM). The clinical negative, NTCs, unamplified master mix with primers, and unamplified plasmid did not show the amplified product. Each sample was analyzed in triplicate with one representative gel image rendering of electropherograms shown here and replicates shown in Fig. S6. (For interpretation of the references to color in this figure legend, the reader is referred to the Web version of this article.)

3.5.2. Recombinase polymerase amplification (RPA)

SARS-CoV-2 RNA was reliably detected from known positive clinical samples via a one-pot reverse transcription RPA (RT-RPA) reaction. Similar to a RT-PCR amplification curve, successful RPA-based identification is represented by a steep increase in fluorescence associated with the onset of exponential amplification. Given that RPA is an isothermal technique, there is no C_t value to measure amplification performance, as used in real-time RT-PCR, but rather a time until measured fluorescence crosses an empirical threshold. All positive extracts prepared by the enriched rnaGEM/PDQeX method displayed such amplification, while the negative clinical sample did not (Fig. 6A).

We concluded that amplification was specific for to the SARS-CoV-2 target since the fluorescent signal was generated via probe hybridization and the NTCs did not amplify. Notably, the average time to amplification for all three clinical samples was similar to or less than that of the cDNA plasmid positive control. Since RPA amplifies DNA and not the viral RNA itself, these results demonstrated the success of the 1-min, in-pot reverse transcription step upstream of amplification (Fig. 6B). All replicates of positive clinical samples displayed amplification following isothermal incubation in approximately 5 min, significantly more rapid than the 30-min amplification required for the PCR-based method, highlighting the potential use for RPA-based ultra-rapid testing.

3.5.3. Colorimetric loop-mediated amplification (LAMP)

For LAMP detection, we employed the colorimetric indicator hydroxynapthol blue (HNB), which changes from a purple to a blue color with nucleic acid amplification, providing a binary metric for the presence of a given target. With eluates produced by our method, all four clinical SARS-CoV-2 positive extracts and dilutions of the plasmid positive control appeared blue in color, indicating successful amplification (Fig. 7A). Conversely, the negative extract and the no template control were purple, indicating assay specificity for the SARS-CoV-2 target.

Despite the possibility for naked-eye interpretation, variations in human perception of color and variable ambient lighting can hinder universal visualization [50]. To mitigate this, we implemented a method for empirical colorimetric analysis based on cellphone image capture and ImageJ freeware [39,51]. By measuring hue, which can be represented as a single numerical value from 0° to 360° on the color wheel [52], monitored amplification via hue analysis over time and quantified the bitonal color change [52]. Hue analysis indicated that amplification occurred in all four positive clinical samples (Fig. 7B) and positive control reactions containing the positive control plasmid, confirming conclusions drawn via visual interpretation (Fig. 7C). At 30 min, two of the positive reactions in clinical samples had measured hue values below the amplification threshold and by 60 min, SARS-CoV-2 RNA had been successfully detected in all known positive extracts (Fig. 7B–C). Additionally, the average hue values for NTCs and the clinical negative increased, moving further into the purple (negative) range. Since the limit of detection of RT-LAMP was expected to be equal to or higher than real-time RT-PCR, this finding was

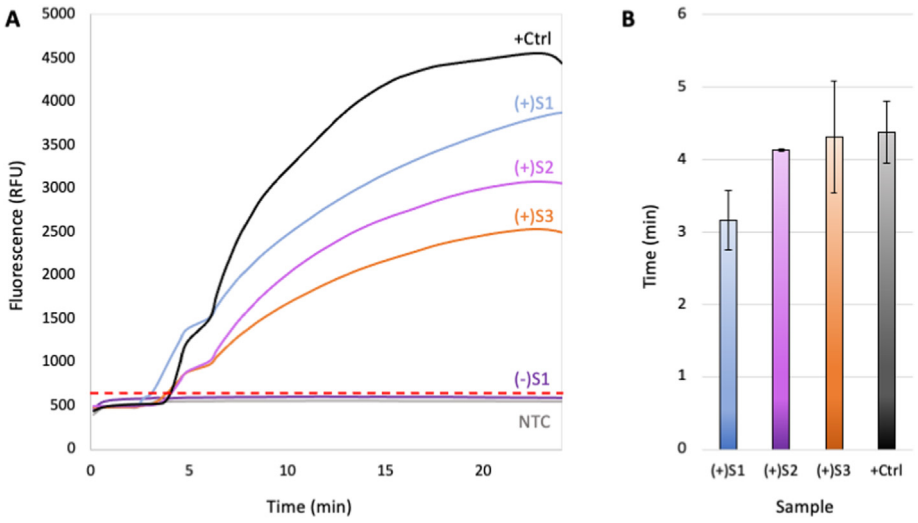

Fig. 6. Reverse Transcription Recombinase Polymerase Amplification (RT-RPA) of extracted SARS-CoV-2 RNA. (A) Amplification plot depicting mean fluorescence of three clinical positives and one clinical negative, along with controls (n = 3). A threshold (618.6187 RFU) for amplification (dotted red line) was calculated as 3 standard deviations above the mean fluorescence of NTCs. SARS-CoV-2 RNA was detected in all three clinical positives, but not in the clinical negative or NTCs. (B) Mean time to amplification was calculated for each sample, with error bars representing one standard deviation in both the positive and negative directions. Clinical positives amplified in the same or less time than the positive control (2019-nCoV_N_Positive Control plasmid, 1000 copies/μL). (For interpretation of the references to color in this figure legend, the reader is referred to the Web version of this article.)

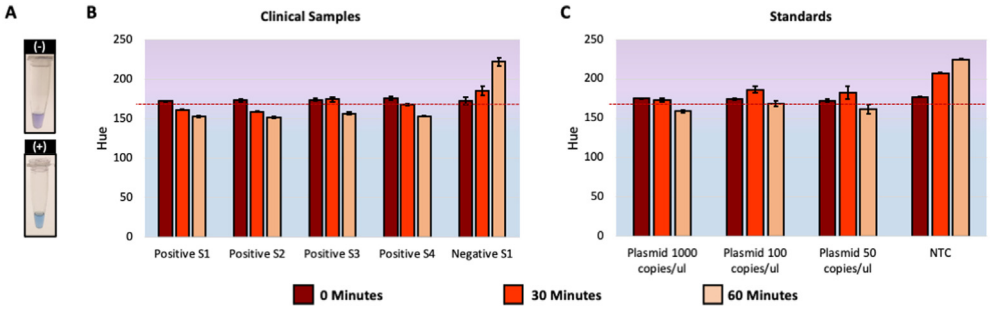

Fig. 7. Detection of viral genomic targets using colorimetric loop-mediated isothermal amplification (LAMP). (A) Depictions of HNB dye as a colorimetric indicator with LAMP; negative reactions were purple and positive reactions were blue. (B) Four clinical positive extracts and one clinical negative were analyzed in triplicate via LAMP and images were captured at 0, 30, and 60 min. Following image analysis, an analytical threshold was calculated (169.52, 3 standard deviations above the mean hue at time = 0). Samples above the threshold (purple) were determined to be negative and samples below the threshold (blue) were positive for the SARS-CoV-2 N1 target. At 30 min, SARS-CoV-2 RNA was detected in two of the four known positives. By 60 min, all four clinical positives were detected. The clinical negative remained purple, indicating that no amplification. (C) Standard solutions of the 2019-nCoV_N_Positive Control plasmid were prepared by serial dilution and amplified along with NTCs. At 60 min, all positive control dilutions were determined to be positive, while NTCs remained negative. (For interpretation of the references to color in this figure legend, the reader is referred to the Web version of this article.)

important in terms of demonstrating that sufficient RNA is liberated via enriched rnaGEM extraction to enable colorimetric RT-LAMP detection [9].

3.6. RNA extraction from saliva samples

Viral detection in saliva possesses comparable sensitivity to nasopharyngeal swabbing for detection of respiratory pathogens, including endemic coronaviruses [53]. However, saliva collection offers the potential for simple, non-invasive at home sampling, which minimizes nosocomial transmission risk, lessens demand for consumables (e.g., swabs and personal protective equipment), decreases cost, shortens turnaround time, and allows for facile repeat testing [53,54]. As such, we assessed the ability of our sample preparation method to prepare amplification-ready RNA directly from saliva. Unfortunately, saliva is a complex and highly viscous matrix, which can cause low analytical efficiency [54]. To mitigate resultant matrix effects, a dilution buffer was mixed with saliva prior to viral preconcentration. We tested three positive clinical samples neat in VTM and serially diluted in the saliva matrix at 2X, 5X, and 10X (Fig. 8). Viral RNA was detected in the neat extracts of all three samples of varying viral titers and a minimum of one saliva dilution for each sample. For the highest titer sample, viral RNA was detected down to a 10X dilution in saliva (Fig. 8A). While this is not directly representative of actual patient sample composition, it nonetheless demonstrates compatibility of our extraction technique with saliva testing.

4. Conclusions

We have demonstrated a simple, rapid method for SARS-CoV-2 viral preconcentration and enzymatic RNA extraction from clinically relevant matrices, including viral transport media (VTM) and saliva, and characterized its use with amplification-based detection. The bandwidth of this approach is highlighted by successful detection of SARS-CoV-2 in neat patient diagnostic remnants, dilutions reminiscent of surveillance samples, and contrived saliva samples — all exhibiting comparable performance to commercial

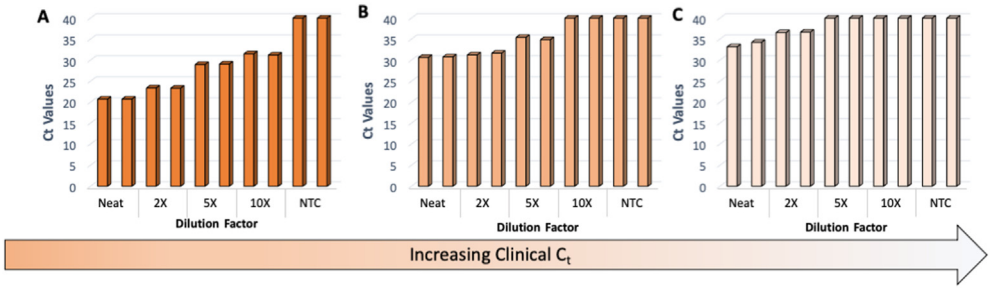

Fig. 8. Compatibility of extraction from saliva matrices. The enriched rnaGEM method was used to extract SARS-CoV-2 RNA from three known clinically positive VTM samples serially diluted in a saliva matrix. Three samples with comparatively (A) low, (B) moderate, and (C) high clinical Ct values were selected to allow for comparison of extraction efficacy across a broad range of samples. The Ct values were used to estimate relative viral titers of these samples. Extracts were analyzed by RT-PCR, each in duplicate. For all three samples, SARS-CoV-2 was detected in at least one sample extracted from a saliva sample.

kit-based SPE. A double-blind RT-PCR study demonstrated 100% concordance with clinical results, clearly the ability of our technique to provide accurate results from real nasopharyngeal (NP) samples. However, since saliva is preferable over NP swabs due to simple, non-invasive collection, readily predisposed to at-home sampling, we also showed our technique's ability to effectively obtain viral RNA from even low-titer samples comprised of up to 90% saliva matrix. SARS-CoV-2 was detected in extract dilutions up to 20X, indicating effective RNA extraction and potential applicability to pooled sampling – essential for epidemiological control, especially in low-prevalence or asymptomatic populations [25]. Our approach combines the advantages of enhanced sensitivity with a rapid, simple workflow imparted by combining rnaGEM extraction chemistry with commercial PDQeX technology to minimize required manual steps; both viral enrichment and extraction of amplification-ready RNA was achieved in under 10 min, making this technique well-suited to applications that mandate short turnaround times.

We established compatibility of our extraction method with a panel of amplification techniques, which may be used for various applications. We observed 100% concordance between qualitative results obtained following microfluidic RT-PCR and known laboratory diagnoses. Although detection was accomplished off-disc, microfluidic electrophoretic fluorescence detection is possible [35,37], which could be coupled with this extraction method for development of an integrated sample-to-result system for *in situ* viral detection, entirely untethered from a centralized laboratory. Similarly, an emerging class of portable, on-site diagnostic tools leverage isothermal amplification techniques due to significantly simplified instrumentation required relative to PCR-based assays. We established compatibility of enriched rnaGEM extracts with two such isothermal methods, recombinase polymerase amplification (RPA) and loop-mediated amplification (LAMP). RPA permitted extremely rapid SARS-CoV-2 identification, with all clinical positive extracts displaying amplification in ~5 min; total turnaround time, including sample preparation, was approximately 15 min – orders of magnitude below the 24–48 h interval associated with conventional laboratory testing. Moreover, RNA extracted using the method described here was successfully detected using colorimetric LAMP, advantageous in terms of supplying simplified visual interpretation, either by eye or with smartphone-based image capture. Finally, it should be apparent to the reader that the methodology reported here is easily modified for microscale integration.

CRediT authorship contribution statement

Leah M. Dignan: Conceptualization, Methodology, Investigation, Data curation, Formal analysis, Visualization, Writing – original draft, Writing – review & editing. **Rachelle Turiello:** Conceptualization, Methodology, Investigation, Data curation, Formal analysis, Visualization, Writing – original draft, Writing – review & editing. **Tiffany R. Layne:** Investigation, Data curation. **Killian C. O'Connell:** Investigation, Data curation. **Jeff Hickey:** Conceptualization, Methodology. **Jeff Chapman:** Funding acquisition, Project administration, Supervision. **Melinda D. Poulter:** Resources. **James P. Landers:** Funding acquisition, Project administration, Supervision, all authors contributed. All authors have read and approved the published version of the manuscript.

Declaration of competing interest

This work was sponsored by MicroGEM USA, will be available to them for licensing from the University of Virginia, and the PI has an equity interest in this entity.

Acknowledgements

We would like to acknowledge MicroGEM International PLC for their expertise and support of this project.

Appendix A. Supplementary data

Supplementary data to this article can be found online at https://doi.org/10.1016/j.aca.2021.338846.

Funding

This work was supported by the National Institutes of Health (Grant Number: 75N92020C00015).

References

[1] N. Zhu, D. Zhang, W. Wang, X. Li, B. Yang, J. Song, X. Zhao, B. Huang, W. Shi, R. Lu, P. Niu, F. Zhan, X. Ma, D. Wang, W. Xu, G. Wu, G.F. Gao, W. Tan, N. Engl. J. Med. 382 (2020) 727–733.
[2] W. Guan, Z. Ni, Y. Hu, W. Liang, C. Ou, J. He, L. Liu, H. Shan, C. Lei, D.S.C. Hui, B. Du, L. Li, G. Zeng, K.-Y. Yuen, R. Chen, C. Tang, T. Wang, P. Chen, J. Xiang, S. Li, J. Wang, Z. Liang, Y. Peng, L. Wei, Y. Liu, Y. Hu, P. Peng, J. Wang, J. Liu, Z. Chen, G. Li, Z. Zheng, S. Qiu, J. Luo, C. Ye, S. Zhu, N. Zhong, N. Engl. J. Med. 382 (2020) 1708–1720.
[3] N. Chen, M. Zhou, X. Dong, J. Qu, F. Gong, Y. Han, Y. Qiu, J. Wang, Y. Liu, Y. Wei, J. Xia, T. Yu, X. Zhang, L. Zhang, Lancet 395 (2020) 507–513.
[4] D.B. Larremore, B.K. Fosdick, K.M. Bubar, S. Zhang, S.M. Kissler, C.J.E. Metcalf, C. Buckee, Y. Grad, Estimating SARS-CoV-2 Seroprevalence and Epidemiological Parameters with Uncertainty from Serological Surveys, Infectious Diseases (except HIV/AIDS), 2020.
[5] M.N. Esbin, O.N. Whitney, S. Chong, A. Maurer, X. Darzacq, R. Tjian, RNA 26 (2020) 771–783.
[6] K. Uhteg, J. Jarrett, M. Richards, C. Howard, E. Morehead, M. Geahr, L. Gluck, A. Hanlon, B. Ellis, H. Kaur, P. Simner, K.C. Carroll, H.H. Mostafa, J. Clin. Virol.

127 (2020) 104384.
[7] D. Fraga, T. Meulia, S. Fenster, Current Protocols Essential Laboratory Techniques 8 (2014), 10.3.1-10.3.40.
[8] T. Notomi, Nucleic Acids Res. 28 (2000) 63e–663.
[9] M. Goto, E. Honda, A. Ogura, A. Nomoto, K.-I. Hanaki, Biotechniques 46 (2009) 167–172.
[10] Y. Zhang, N. Odiwuor, J. Xiong, L. Sun, R.O. Nyaruaba, H. Wei, N.A. Tanner, Rapid Molecular Detection of SARS-CoV-2 (COVID-19) Virus RNA Using Colorimetric LAMP, Infectious Diseases (except HIV/AIDS), 2020.
[11] W.E. Huang, B. Lim, C. Hsu, D. Xiong, W. Wu, Y. Yu, H. Jia, Y. Wang, Y. Zeng, M. Ji, H. Chang, X. Zhang, H. Wang, Z. Cui, Microb. Biotechnol. 13 (2020) 950–961.
[12] G.-S. Park, K. Ku, S.-H. Baek, S.-J. Kim, S.I. Kim, B.-T. Kim, J.-S. Maeng, J. Mol. Diagn. 22 (2020) 729–735.
[13] V.L. Dao Thi, K. Herbst, K. Boerner, M. Meurer, L.P. Kremer, D. Kirrmaier, A. Freistaedter, D. Papagiannidis, C. Galmozzi, M.L. Stanifer, S. Boulant, S. Klein, P. Chlanda, D. Khalid, I. Barreto Miranda, P. Schnitzler, H.-G. Kräusslich, M. Knop, S. Anders, Sci. Transl. Med. 12 (2020), eabc7075.
[14] M.J. Kellner, J.J. Ross, J. Schnabl, M.P.S. Dekens, R. Heinen, I. Grishkovskaya, B. Bauer, J. Stadlmann, L. Menéndez-Arias, R. Fritsche-Polanz, M. Traugott, T. Seitz, A. Zoufaly, M. Födinger, C. Wenisch, J. Zuber, , Vienna Covid-19 Diagnostics Initiative (VCDI), A. Pauli, J. Brennecke, A Rapid, Highly Sensitive and Open-Access SARS-CoV-2 Detection Assay for Laboratory and Home Testing, Molecular Biology, 2020.
[15] O. Piepenburg, C.H. Williams, D.L. Stemple, N.A. Armes, PLoS Biol. 4 (2006), e204.
[16] I.M. Lobato, C.K. O'Sullivan, Trac. Trends Anal. Chem. 98 (2018) 19–35.
[17] R.K. Daher, G. Stewart, M. Boissinot, M.G. Bergeron, Clin. Chem. 62 (2016) 947–958.
[18] F. Ahmad, S.A. Hashsham, Anal. Chim. Acta 733 (2012) 1–15.
[19] A.A. El Wahed, P. Patel, M. Maier, C. Pietsch, D. Rüster, S. Böhlken-Fascher, J. Kissenkötter, O. Behrmann, M. Frimpong, M.M. Diagne, M. Faye, N. Dia, M.A. Shalaby, H. Amer, M. Elgamal, A. Zaki, G. Ismail, M. Kaiser, V.M. Corman, M. Niedrig, O. Landt, O. Faye, A.A. Sall, F.T. Hufert, U. Truyen, U.G. Liebert, M. Weidmann, Anal. Chem. (2021), 0c04779 acs.analchem.
[20] Y.-W. Tang, J.E. Schmitz, D.H. Persing, C.W. Stratton, J. Clin. Microbiol. 58 (2020) e00512–e00520. /jcm/58/6/JCM.00512-20.atom.
[21] N. Ali, R. de C.P. Rampazzo, A.D.T. Costa, M.A. Krieger, BioMed Res. Int. (2017) 1–13, 2017.
[22] R.A. Barclay, I. Akhrymuk, A. Patnaik, V. Callahan, C. Lehman, P. Andersen, R. Barbero, S. Barksdale, R. Dunlap, D. Goldfarb, T. Jones-Roe, R. Kelly, B. Kim, S. Miao, A. Munns, D. Munns, S. Patel, E. Porter, R. Ramsey, S. Sahoo, O. Swahn, J. Warsh, K. Kehn-Hall, B. Lepene, Sci. Rep. 10 (2020) 22425.
[23] V. M. Corman, O. Landt, M. Kaiser, R. Molenkamp, A. Meijer, D. K. Chu, T. Bleicker, S. Brünink, J. Schneider, M. L. Schmidt, D. G. Mulders, B. L. Haagmans, B. van der Veer, S. van den Brink, L. Wijsman, G. Goderski, J.-L. Romette, J. Ellis, M. Zambon, M. Peiris, H. Goossens, C. Reusken, M. P. Koopmans and C. Drosten, Euro Surveill., , DOI:10.2807/1560-7917.ES.2020.25.3.2000045.
[24] S. Lohse, T. Pfuhl, B. Berkó-Göttel, J. Rissland, T. Geißler, B. Gärtner, S.L. Becker, S. Schneitler, S. Smola, Lancet Infect. Dis. 20 (2020) 1231–1232.
[25] Report to congress: COVID-19 strategic testing plan. https://www.democrats.senate.gov/imo/media/doc/COVID%20Nat ional%20Diagnostics%20Strategy%2005%2024%202020%20v%20FINAL.pdf, 2020. (Accessed 25 January 2021).
[26] A. Luchini, D.H. Geho, B. Bishop, D. Tran, C. Xia, R.L. Dufour, C.D. Jones, V. Espina, A. Patanarut, W. Zhou, M.M. Ross, A. Tessitore, E.F. Petricoin, L.A. Liotta, Nano Lett. 8 (2008) 350–361.
[27] R. Barclay, I. Akhrymuk, A. Patnaik, V. Callahan, C. Lehman, P. Andersen, R. Barbero, S. Barksdale, R. Dunlap, D. Goldfarb, T. Jones-Roe, R. Kelly, B. Kim, S. Miao, A. Munns, D. Munns, S. Patel, E. Porter, R. Ramsey, S. Sahoo, O. Swahn, J. Warsh, K. Kehn-Hall, B. Lepene, Nanotrap ® particles improve detection of SARS-CoV-2 for pooled sample methods, extraction-free saliva methods, and extraction-free transport medium methods, Microbiology (2020), https://doi.org/10.1101/2020.06.25.172510.
[28] K.J. Morrow Jr., Genet. Eng. Biotechnol. news 31 (2011), 1-24–26.
[29] J.A. Lounsbury, N. Coult, D.C. Miranian, S.M. Cronk, D.M. Haverstick, P. Kinnon, D.J. Saul, J.P. Landers, Forensic Sci. Int.: Genetics 6 (2012) 607–615.
[30] D. Moss, S.-A. Harbison, D.J. Saul, Int. J. Leg. Med. 117 (2003) 340–349.
[31] D.B. Larremore, B. Wilder, E. Lester, S. Shehata, J.M. Burke, J.A. Hay, M. Tambe, M.J. Mina, R. Parker, Test Sensitivity Is Secondary to Frequency and Turnaround Time for COVID-19 Surveillance, Infectious Diseases (except HIV/AIDS), 2020.
[32] M.J. Mina, R. Parker, D.B. Larremore, N. Engl. J. Med. (2020), NEJMp2025631.
[33] J. Hadaya, M. Schumm, E.H. Livingston, J. Am. Med. Assoc. 323 (2020) 1981.
[34] B.L. Thompson, Y. Ouyang, G.R.M. Duarte, E. Carrilho, S.T. Krauss, J.P. Landers, Nat. Protoc. 10 (2015) 875–886.
[35] C. Birch, J. DuVall, D. Le Roux, B. Thompson, A.-C. Tsuei, J. Li, D. Nelson, D. Mills, J. Landers, B. Root, Micromachines 8 (2017) 17.
[36] J.L. Garcia-Cordero, D. Kurzbuch, F. Benito-Lopez, D. Diamond, L.P. Lee, A.J. Ricco, Lab Chip 10 (2010) 2680.
[37] A. Scott, D. Mills, C. Birch, S. Panesar, J. Li, D. Nelson, M. Starteva, A. Khim, B. Root, J.P. Landers, Lab Chip 19 (2019) 3834–3843.
[38] O. Behrmann, I. Bachmann, M. Spiegel, M. Schramm, A. Abd El Wahed, G. Dobler, G. Dame, F.T. Hufert, Clin. Chem. 66 (2020) 1047–1054.
[39] K.R. Jackson, T. Layne, D.A. Dent, A. Tsuei, J. Li, D.M. Haverstick, J.P. Landers, Forensic Sci. Int.: Genetics 45 (2020) 102195.
[40] M. S. Woolf, L. M. Dignan, A. T. Scott and J. P. Landers, Nature Protocols.
[41] Real-time PCR: understanding Ct. https://www.thermofisher.com/us/en/home/life-science/pcr/real-time-pcr/real-time-pcr-learning-center/real-time-pcr-basics/real-time-pcr-understanding-ct.htmlR accessed October 15, 2020.
[42] J. Bullard, K. Dust, D. Funk, J.E. Strong, D. Alexander, L. Garnett, C. Boodman, A. Bello, A. Hedley, Z. Schiffman, K. Doan, N. Bastien, Y. Li, P.G. Van Caeseele, G. Poliquin, Clin. Infect. Dis. (2020), ciaa638.
[43] RNA Isolation for qRT-PCR. https://www.thermofisher.com/us/en/home/references/ambion-tech-support/rtpcr-analysis/general-articles/rna-isolation-for-qrt-pcr.html. (Accessed 15 October 2020).
[44] H. Laurell, J.S. Iacovoni, A. Abot, D. Svec, J.-J. Maoret, J.-F. Arnal, M. Kubista, Nucleic Acids Res. 40 (2012) e51–e51.
[45] V.J. Gadkar, M. Filion, BMC Biotechnol. 13 (2013) 7.
[46] J. Norhazlin, M.N.K. Nor-Ashikin, B.P. Hoh, S.H. Sheikh Abdul Kadir, S. Norita, M. Mohd-Fazirul, W.J. Wan-Hafizah, D. Razif, M.H. Rajikin, B. Abdullah, Genet. Mol. Res. 14 (2015) 10172–10184.
[47] M.J. Madou, G.J. Kellogg (Eds.), G. E. Cohn, 1998, pp. 80–93. San Jose, CA.
[48] R. Gorkin, J. Park, J. Siegrist, M. Amasia, B.S. Lee, J.-M. Park, J. Kim, H. Kim, M. Madou, Y.-K. Cho, Lab Chip 10 (2010) 1758.
[49] Y. Zhang, P. Ozdemir, Anal. Chim. Acta 638 (2009) 115–125.
[50] J. Liu, Z. Shao, Q. Cheng, Opt. Lett. 36 (2011) 4821.
[51] A. Scott, K. Jackson, M. Carter, R. Comeau, T. Layne, J. Landers, Forensic Sci. Int.: Genetics 43 (2019) 102139.
[52] K. Cantrell, M.M. Erenas, I. de Orbe-Payá, L.F. Capitán-Vallvey, Anal. Chem. 82 (2010) 531–542.
[53] A.L. Wyllie, J. Fournier, A. Casanovas-Massana, M. Campbell, M. Tokuyama, P. Vijayakumar, B. Geng, M.C. Muenker, A.J. Moore, C.B.F. Vogels, M.E. Petrone, I.M. Ott, P. Lu, A. Lu-Culligan, J. Klein, A. Venkataraman, R. Earnest, M. Simonov, R. Datta, R. Handoko, N. Naushad, L.R. Sewanan, J. Valdez, E.B. White, S. Lapidus, C.C. Kalinich, X. Jiang, D.J. Kim, E. Kudo, M. Linehan, T. Mao, M. Moriyama, J.E. Oh, A. Park, J. Silva, E. Song, T. Takahashi, M. Taura, O.-E. Weizman, P. Wong, Y. Yang, S. Bermejo, C. Odio, S.B. Omer, C.S. Dela Cruz, S. Farhadian, R.A. Martinello, A. Iwasaki, N.D. Grubaugh, A.I. Ko, Saliva Is More Sensitive for SARS-CoV-2 Detection in COVID-19 Patients than Nasopharyngeal Swabs, Infectious Diseases (except HIV/AIDS), 2020.
[54] F. Wei, D.T.W. Wong, Chin. J. Dent. Res. 15 (2012) 7–15.